Journal of Plant Physiology 321 (2026) 154773

Contents lists available at ScienceDirect

Journal of Plant Physiology

journal homepage: www.elsevier.com/locate/jplph

Extracellular ROS perception by HPCA1 sustains wound-induced systemic signaling and stomatal closure at the cotyledon stage in Arabidopsis

I. Fraudentali [a,*], A. Furlani [a], M. Gagliano [a], A. Cona [a,b]

[a] Department of Science, Roma Tre University, Viale Guglielmo Marconi 446, 00146, Rome, Italy
[b] Interuniversity Consortium INBB National Institute of Biostructures and Biosystems, 00136, Rome, Italy

ARTICLE INFO

Keywords:
HPCA1
Reactive oxygen species
Systemic signaling
Stomatal closure
Arabidopsis thaliana seedlings
Wounding

ABSTRACT

HPCA1 is a plasma membrane-localized H_2O_2 receptor that has been implicated in extracellular ROS perception and calcium signaling, yet its role in systemic propagation of rapid signals and acclimation responses remains unclear. Here, we investigated the role of HPCA1 in wound-induced systemic ROS signaling and stomatal regulation in 7-day-old *Arabidopsis thaliana* seedlings. Using *in vivo* fluorescence imaging with the ROS-sensitive probe CM-H_2DCFDA, we show that mechanical injury applied to either cotyledons or roots triggers a rapid and sustained systemic ROS accumulation in wild-type seedlings. In contrast, this response is impaired in *hpca1*, indicating that HPCA1 is required to sustain wound-induced systemic ROS signaling in seedlings. Consistently, loss of HPCA1 compromised ROS accumulation in guard cells following both wounding and exogenous H_2O_2 treatment. This deficiency is associated with the complete loss of local and distal stomatal closure, whereas wild-type seedlings display consistent and coordinated stomatal responses. These results indicate that extracellular ROS perception mediated by HPCA1 is essential for the transduction of systemic ROS signals into a functional physiological acclimation response at the guard-cell level. Altogether, our findings support a model in which HPCA1 acts as a key hub coupling extracellular ROS perception with signal propagation and intracellular transduction pathways, thereby sustaining wound-induced systemic signaling and coordinating stomatal acclimation in Arabidopsis seedlings.

1. Introduction

Plants are sessile organisms exposed to highly dynamic environments and have therefore developed sophisticated strategies to rapidly sense, integrate, and respond to external changes. Selective pressure imposed by different biotic and abiotic stresses has shaped plant signaling systems to perceive local stimuli and transmit signals throughout the organism, ultimately coordinating systemic cellular, physiological, and morphological responses (Paes de Melo et al., 2022). These systemic signals promote recovery and survival through acclimation processes, which are reversible adjustments based on phenotypic plasticity (Kouhen et al., 2023). A variety of signals travel within plants, such as hormones, metabolites, and peptides. More recently, rapid long-distance signals have been identified, including hydraulic waves, electrical signals, calcium (Ca^{2+}) waves, and reactive oxygen species (ROS)-mediated signals (Johns et al., 2021; Peláez-Vico et al., 2022).

ROS have long been considered harmful byproducts of aerobic metabolism; yet they play key physiological roles at low concentrations, such as defense against pathogens and systemic signaling in plants (Mansoor et al., 2022; Wang et al., 2024). Compared to other ROS, hydrogen peroxide (H_2O_2) is well suited as a mobile signal, due to its relatively long half-life (~1 ms), lower reactivity, and reduced toxicity at low concentrations (Wang and Song, 2008). In plants, one of the main sources of apoplastic ROS is the plasma membrane (PM)-localized NADPH oxidases Respiratory Burst Oxidase Homologs (RBOHs). Particularly, RBOHD and RBOHF isoforms have been identified as key mediators in response to wounding (Morales et al., 2016; Zandalinas et al., 2020; Fraudentali et al., 2023). Following stress perception, RBOHs catalyze the oxidation of molecular oxygen to superoxide anion ($O_2^{\bullet-}$), which is rapidly converted into H_2O_2 spontaneously or by extracellular superoxide dismutase (SOD; Peláez-Vico et al., 2024). Apoplastic ROS can either remain in the extracellular space or enter plant cells, altering their redox state and reacting with numerous target proteins (Mittler and Jones, 2024).

While long-distance ROS signaling has been extensively investigated (Lew et al., 2020; Zandalinas et al., 2020; Terrón-Camero et al., 2022),

* Corresponding author.
E-mail address: ilaria.fraudentali@uniroma3.it (I. Fraudentali).

https://doi.org/10.1016/j.jplph.2026.154773
Received 29 January 2026; Received in revised form 1 April 2026; Accepted 16 April 2026
Available online 16 April 2026

less is known about the molecular components involved in decoding the ROS burst, specifically proteins that perceive apoplastic ROS and mediate cross-talk with other signaling pathways (Planas-Riverola et al., 2021; Myers et al., 2024). In this context, the first PM-localized sensor for apoplastic H_2O_2, the Hydrogen Peroxide-induced Ca^{2+} increases 1 (HPCA1) receptor, has recently been characterized. This protein was originally observed in *Arabidopsis thaliana* stomata guard cells, but homologs were recently reported also in *Oryza sativa* (Wu et al., 2020; Guo et al., 2024). HPCA1 is a leucine-rich repeat receptor kinase (LRR-RK) with an extracellular domain harboring two cysteine pairs, and an intracellular kinase domain. Oxidation of the cysteines' thiol groups by apoplastic H_2O_2 converts Cys-S^- into sulfenic acid (Cys-SOH), inducing a conformational change that promotes HPCA1 auto-phosphorylation and the subsequent activation of its kinase activity (Wu et al., 2020; Planas-Riverola et al., 2021). In Arabidopsis seedlings, *HPCA1* is widely expressed across vegetative tissues, indicating that its role may extend beyond guard-cell signaling (Wu et al., 2020). This broad expression pattern prompts the question of whether HPCA1 contributes to systemic ROS signals initiation and propagation.

In addition to the specific role of HPCA1 in long-distance signaling, the molecular targets of its kinase activity also remain largely unknown. To date, experimental evidence suggested that HPCA1 may interact with Ca^{2+}-permeable channels, among which is Mechanosensitive ion channel Like 3 (MSL3). Consistently, a lower increase in cytosolic calcium concentrations ($[Ca^{2+}]_{cyt}$) has been observed in Arabidopsis *hpca1* lines after exogenous H_2O_2 treatment (Wu et al., 2020), and in response to high light (HL) stress (Fichman et al., 2022). A similar phenotype was also found in *msl3* mutant lines, suggesting that the Ca^{2+} channel MSL3 acts downstream of, and may be activated by, HPCA1. Moreover, it has been shown that HPCA1 is not essential for electrical signaling, as *hpca1* mutants display unaltered PM depolarization upon stress. In detail, under HL stress conditions, *hpca1* lines exhibited impaired ROS and Ca^{2+} accumulation, while electrical signals remained unaffected. These findings indicate that HPCA1 functions as a specific hub coupling Ca^{2+}- and ROS-mediated systemic signals, operating independently from rapid electrical signaling pathways (Fichman et al., 2022). In addition, in adult Arabidopsis leaves, HPCA1 was shown to be required for systemic ROS and Ca^{2+} signaling in response to various abiotic and biotic stresses, including HL and pathogen attack; however, wound-induced systemic ROS signal propagation was reported to occur largely independently of HPCA1 (Fichman et al., 2022).

ROS and Ca^{2+} signals are functionally interconnected through an auto-propagating feedback loop between apoplastic ROS production and Ca^{2+} influx, which enables cell-to-cell propagation of stress signals (Miller et al., 2009). This tight coupling underlies the systemic coordination of acclimation responses, including hormone biosynthesis, defense activation, and stomata regulation (Fichman and Mittler, 2020; Peláez-Vico et al., 2022, 2024).

Stomatal closure is one of the best-characterized acclimation responses to a plethora of stress (Lawson and Matthews, 2020; Rodrigues and Shan, 2022). For instance, mechanical wounding induces a rapid systemic stomatal acclimation response, detectable within minutes after stress perception, helping to regulate transpiration rates and limit pathogen entrance (Devireddy et al., 2020; Fraudentali et al., 2023). Stress-induced stomatal closure is mediated by the phytohormones jasmonic acid (JA) and abscisic acid (ABA), both triggering apoplastic ROS production and accumulation, and subsequent increases in $[Ca^{2+}]_{cyt}$ leading to turgor loss in guard cells (Fraudentali et al., 2020; Liu et al., 2022; Rodrigues and Shan, 2022; Ladeynova et al., 2023).

Considering that HPCA1 is especially localized in guard cells (Wu et al., 2020), and implicated in ROS-mediated signals (Fichman et al., 2022), we investigated its potential role in systemic wound signaling and in the implementation of stomata closure as part of the acclimation response. To address this question, we analyzed systemic ROS accumulation in Arabidopsis *hpca1* mutant seedling subjected to wounding. ROS dynamics were monitored *in vivo* during signal propagation across cotyledons using fluorescence imaging, while ROS accumulation in guard cells was independently quantified by confocal microscopy. Stomatal closure was evaluated as a physiological marker of the acclimation response to wounding. Since HPCA1 appears dispensable for wound-induced systemic ROS signaling in adult leaves (Fichman et al., 2022), we focused on the cotyledonary stage to investigate whether HPCA1 may play a distinct and potentially more central role during early plant development.

2. Materials & methods

2.1. Plant materials, growth conditions and treatments

The *Arabidopsis thaliana* Columbia-0 (Col-0) ecotype was used as the wild-type (WT). The Col-0 T-DNA insertion line for *HPCA1* (At5g49760; TAIR accession no. 2157041), referred to as *hpca1* (CS923304), was generated by Prof. Zhen Ming Pei (Department of Biology, Duke University, Durham, NC, USA; Wu et al., 2020) and kindly provided to us by Prof. Alex Costa (Department of Biosciences, University of Milan, Milan, Italy). Plants were cultured in a growth chamber at 23 °C under long-day conditions (16/8 h photoperiod; 150 μmol m^{-2} s^{-1} and 55% relative humidity). Prior to *in vitro* culture, seeds of both genotypes were surface-sterilized and stratified in the dark at 4 °C for 48 h; subsequently, they were sown in ½ Murashige and Skoog (MS) salt mixture (pH 5.7) supplemented with 0.5% (w/v) sucrose, and 0.8% (w/v) agar (only in solid medium; Murashige and Skoog, 1962). For all experiments, after 6 days of growth, seedlings were transferred to multiwell plates containing liquid medium and incubated for 24 h under controlled conditions to allow acclimation. Subsequently, 7-day-old seedlings were subjected to either leaf or root wounding, or treated with 100 μM H_2O_2 by direct addition to the liquid medium, depending on the experimental design. Control seedlings were maintained in liquid medium**.** Whole-cotyledon ROS accumulation was analyzed upon leaf or root wounding in 7-day-old WT and *hpca1* seedlings. Stomatal regulation and ROS accumulation in guard cells were assessed in 7-day-old WT and *hpca1* seedlings under control conditions, after leaf or root wounding, and following exogenous treatment with 100 μM H_2O_2. To perform cotyledonary-leaf wounding for measurement of stomatal closure and ROS detection in guard cells, one of two cotyledons was wounded with sterilized scissors, reaching the midvein. For *in vivo* wide-field stereomicroscopy analysis of ROS accumulation, wounding was achieved by injuring one cotyledon with a clean cut, using sterilized scissors. For all experiments, root wounding was performed by gently squeezing the primary root with sterilized tweezers. Unwounded seedlings were used as controls. For exogenous H_2O_2 application, seedlings were immersed in liquid medium supplemented with 100 μM H_2O_2.

2.2. In vivo wide-field stereomicroscopy analysis of ROS accumulation

ROS accumulation in whole-cotyledonary leaves was visualized *in vivo* using the fluorescent probe 2′,7′-dichlorodihydrofluorescein diacetate (CM-H_2DCFDA; Molecular Probes, Invitrogen). Following the acclimation period of 24 h in liquid medium, 7-day-old WT and *hpca1* seedlings were incubated with 10 μM CM-H_2DCFDA for 30 min at room temperature (RT). After incubation, excess dye was removed by rinsing twice with fresh liquid medium. Seedlings were then placed on a growth plate containing solid medium and allowed to acclimate for 20 min. Subsequently, seedlings were exposed to the filtered light of the fluorescence stereomicroscope and left for 5 min for further acclimation. After this period, seedlings were either left intact (control) or subjected to leaf or root wounding. Time-lapse acquisition began immediately before wounding and continued for 45 min, with one frame acquired every 30 s. Imaging was performed using a Zeiss AXIO Zoom.V16 fluorescence stereomicroscope equipped with a Zeiss Axiocam 305 color digital camera. Excitation light was provided by a Zeiss HXP 120 V mercury lamp using a Zeiss 38 HE filter cube [excitation: BP 470/40

(HE); emission: BP 525/50 (HE)]. Each frame was analyzed with ImageJ software by selecting a Region of Interest (ROI) around both cotyledons and in the background. Mean gray values were extracted for each ROI, and background fluorescence was subtracted from the corresponding cotyledon values in every frame. Fluorescence emission intensity (F) obtained over time was normalized to the mean gray value before wounding (F_0) and to the total cotyledon area (A), according to the following formula:

$$\textit{Normalized Fluorescence}\ (\Delta F / A) = \frac{F - F_0}{A}$$

Normalized fluorescence values were plotted over time. Statistical analyses were performed to compare fluorescence values at 1 min, 30 min, and 45 min post-wounding within each genotype and treatment, as well as among different genotypes.

2.3. Measurement of stomatal closure

Stomatal aperture levels were measured as previously described (Shang et al., 2016), with slight modifications (Fraudentali et al., 2023). Following the acclimation period of 24 h in liquid medium, to induce stomatal opening 7-day-old WT and *hpca1* seedlings were incubated in opening solution [30 mM KCl and 10 mM MES-Tris (pH 6.15)] for 3 h under light conditions. Subsequently, the opening solution was replaced with liquid medium containing the appropriate treatments, according to the following experimental conditions: leaf wounding; root wounding; 100 μM H_2O_2. For leaf wounding, stomatal aperture was evaluated both on the wounded cotyledon (local response) and on the unwounded cotyledon (distal response). For time-course analysis, seedlings were observed at 5 min, 15 min, 1 h, 3 h, and 24 h after treatment. At each time point, samples were incubated in a fixing solution [1% (v/v) glutaraldehyde, 10 mM NaPi (pH 7.0), 5 mM $MgCl_2$, and 5 mM EDTA] for 30 min under light conditions. Stomatal pore images were acquired with a Zeiss Axiophot 2 microscope equipped with a Leica DFC450C digital camera at 20× magnification. Stomatal width and length were quantified using ImageJ software and the aperture levels were expressed as width/length ratio. Importantly, stomatal aperture measurements were performed exclusively on fully developed stomata, identified by the presence of two clearly differentiated guard cells and a visible pore (Fig. S2A). Although fully differentiated stomata at this developmental stage may vary in size, all stomata included in the analysis were considered mature and functionally competent. To further assess whether stomatal size influenced the response, stomata were grouped based on guard cell pair length into bigger (>11.5 μm) and smaller (<11.5 μm), and stomatal aperture of each group was expressed as width/length ratio in WT and *hpca1* seedlings in control condition and 1 h after 100 μM H_2O_2 treatment (Fig. S2C), selected as representative conditions to illustrate this analysis.

2.4. In situ detection of ROS in guard cells

ROS accumulation in guard cells was visualized *in vivo* using the fluorescent probe CM-H_2DCFDA (Molecular Probes, Invitrogen), as previously reported (Fraudentali et al., 2023). Following the acclimation period of 24 h in liquid medium, to induce stomatal opening 7-day-old WT and *hpca1* seedlings were incubated in opening solution for 3 h under light conditions. Subsequently, 10 μM CM-H_2DCFDA was added to the opening solution, and samples were incubated for 30 min at RT. Afterwards, excess dye was removed by rinsing twice with fresh liquid medium. Seedlings were then placed in liquid medium containing the appropriate treatments, according to the following experimental conditions: leaf wounding; root wounding; 100 μM H_2O_2. Samples were incubated under light conditions for 5 min or 1 h before visualization. Images were captured using Laser Scanning Confocal Microscopy (LSCM) on a Leica TCS-SP5 equipped with an Argon laser [Excitation: 492–495 nm; Emission: 517–527 nm (CM-H_2DCFDA), 650–700 nm (chlorophyll auto-fluorescence)] and the Leica Application Suite Advanced Fluorescence (LAS-AF; Leica Microsystems, Weltzar, Germany) software. Composite images were generated by merging bright-field, CM-H_2DCFDA, and chlorophyll fluorescence channels. Relative fluorescence intensity of guard cells was quantified using ImageJ software by selecting a ROI and measuring the mean pixel intensity in the green fluorescence channel. Data were expressed as means ± SEM of pixel intensities.

2.5. Statistics

Wide-field fluorescence stereomicroscopy analyses of CM-H_2DCFDA in cotyledons were performed on seedlings from three independent experimental replicates for both leaf and root wounding in each genotype. For each experiment, four seedlings were observed for each genotype and condition. Each of the four seedlings from the three independent experiments was considered as an individual biological replicate ($n = 12$). Images shown here were selected from a single representative experiment.

Stomatal aperture measurements were performed in three independent experimental replicates for each treatment and genotype. For every treatment and time point, five leaves of comparable size were collected from distinct seedlings of each genotype. Each of the five leaves from the three independent experiments was considered as an individual biological replicate, resulting in a total of 15 biological replicates for each genotype and treatment ($n = 15$). For each leaf, four random microscopic fields (430 μm × 325 μm) were selected and at least 60 stomata pores were measured. Mean stomatal aperture values were calculated and used for statistical analysis.

In situ confocal microscopy analysis of CM-H_2DCFDA fluorescence in guard cells was performed on seedlings from three independent experimental replicates for each treatment and genotype. For each experiment, five leaves of comparable size were collected from distinct seedlings for each genotype. Each of the five leaves from the three independent experiments was considered as an individual biological replicate ($n = 15$). For each leaf, five random fields were selected and at least 60 stomata were measured. The images shown here were selected from a single representative experiment.

Statistical analyses were conducted using GraphPad Prism (GraphPad Software) with one-way ANOVA followed by Dunnett's test for comparisons within each genotype, and statistical significance from this analysis is indicated by asterisks (*). Unpaired Student's t-tests were used for comparisons between genotypes under the same conditions, and these are indicated by open circles (°). Significance levels were expressed using p levels as follows: *, $^\circ p \leq 0.05$; **, $^\circ p \leq 0.01$; ***, $^\circ p \leq 0.001$; ****, $^\circ p \leq 0.0001$; if not reported, differences were not statistically significant. Detailed statistical results for all analyzed comparisons are reported in Supplementary materials (Table S1), including mean differences, 95% confidence intervals, and exact p-values.

3. Results

3.1. HPCA1 contributes to wound-induced systemic ROS accumulation in Arabidopsis seedlings

Systemic ROS signals triggered by mechanical injury propagate rapidly from the wounded site to distal tissues, contributing to the coordination of whole-plant stress responses (Devireddy et al., 2020; Fichman and Mittler, 2021; Fraudentali et al., 2023). Given that HPCA1 functions as a PM H_2O_2 sensor linking extracellular ROS perception to intracellular Ca^{2+} signaling, we investigated whether HPCA1 contributes to the initiation and/or maintenance of wound-induced systemic ROS accumulation. To this end, ROS dynamics were monitored *in vivo* in 7-day-old WT and *hpca1* seedlings subjected to cotyledonary-leaf or root wounding, using the fluorescent probe CM-H_2DCFDA, while unwounded seedlings served as controls (Figs. 1 and 2).

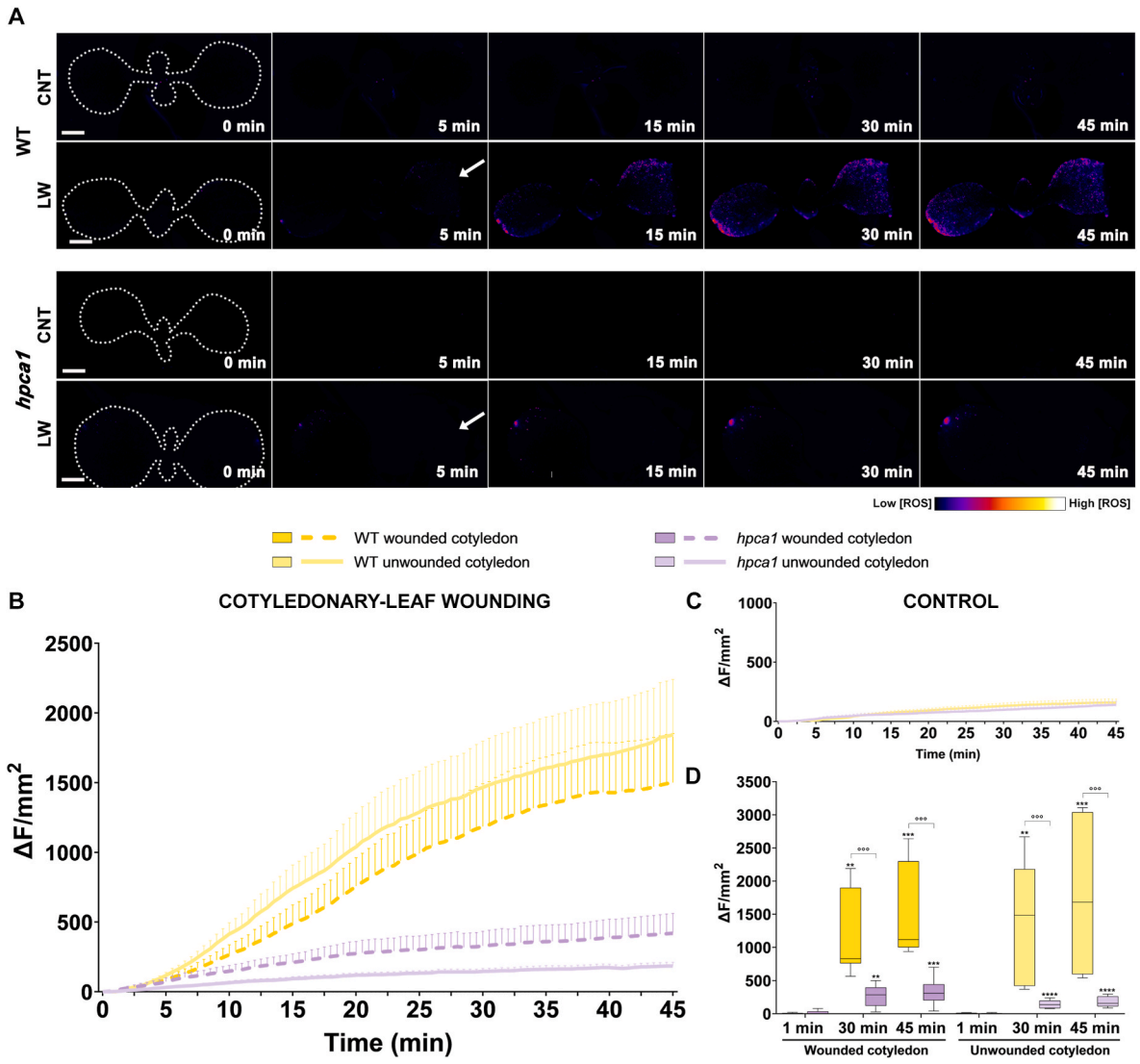

Fig. 1. Systemic ROS accumulation in response to cotyledonary-leaf wounding (LW) in WT and *hpca1* Arabidopsis seedlings. (A) Seedlings were subjected to cotyledonary-leaf wounding and ROS levels were imaged *in vivo* using CM-H_2DCFDA probe and wide-field fluorescence stereomicroscopy. Representative false-color images of control and wounded conditions are shown, at 0, 5, 15, 30 and 45 min after injury. Time-lapse acquisition was performed every 30 s for a total duration of 45 min. Arrows indicate wounded cotyledons. Scale bar = 1 mm. (B, C) Quantification of fluorescence levels, expressed as $\Delta F/mm^2$, over time in both wounded and unwounded cotyledons of seedlings (B) and in control conditions (C). (D) Statistical analysis of ROS accumulation in wounded and unwounded cotyledons at 1, 30 and 45 min post-injury. Median values are reported in the boxplot, as well as minimum and maximum values ($n = 12$). Comparisons within each genotype versus 1 min baseline were performed by one-way ANOVA followed by Dunnett's test (indicated by *), while between-genotype comparisons at the same time point and cotyledon were performed using unpaired *t*-test (indicated by °). Significant levels are reported: $^{**}p \leq 0.01$; ***, $^{\circ}p \leq 0.001$; $^{****}p \leq 0.0001$. Non-significant differences are not shown. (For interpretation of the references to color in this figure legend, the reader is referred to the Web version of this article.)

In WT seedlings, cotyledonary-leaf wounding induced a rapid increase in ROS-associated fluorescence in the injured cotyledon, which progressively extended to the distal, unwounded cotyledon, reaching maximal levels within 45 min after injury (Fig. 1). A comparable systemic pattern was observed following root wounding, with both cotyledons exhibiting a synchronous and sustained increase in fluorescence over time (Fig. 2). These observations confirm that mechanical damage triggers a robust and spatially coordinated ROS accumulation in Arabidopsis seedlings, independently of the site of injury.

In *hpca1* mutant seedlings, wound-induced ROS accumulation was significantly compromised compared to WT following either cotyledonary-leaf or root wounding, both at the local and systemic level (Figs. 1 and 2). Quantitative analyses revealed that, following cotyledonary-leaf wounding, ROS levels in *hpca1* seedlings showed a detectable increase but remained significantly lower than those observed in wounded WT seedlings throughout the entire time-course (Fig. 1), whereas no detectable fluorescence was observed after root wounding (Fig. 2), indicating a severe impairment in wound-induced ROS accumulation. The altered ROS response observed in distal tissues further supports the conclusion that HPCA1 is required for the proper establishment and/or amplification of systemic ROS signals following mechanical injury.

Taken together, these results demonstrate that HPCA1 plays a crucial role in wound-induced systemic ROS accumulation in Arabidopsis seedlings. Unlike components that modulate downstream Ca^{2+} dynamics without affecting ROS levels, the loss of HPCA1 compromises the ROS signal itself, supporting a model in which extracellular ROS perception by HPCA1 is necessary to sustain the ROS amplification processes underlying long-distance signaling after wounding.

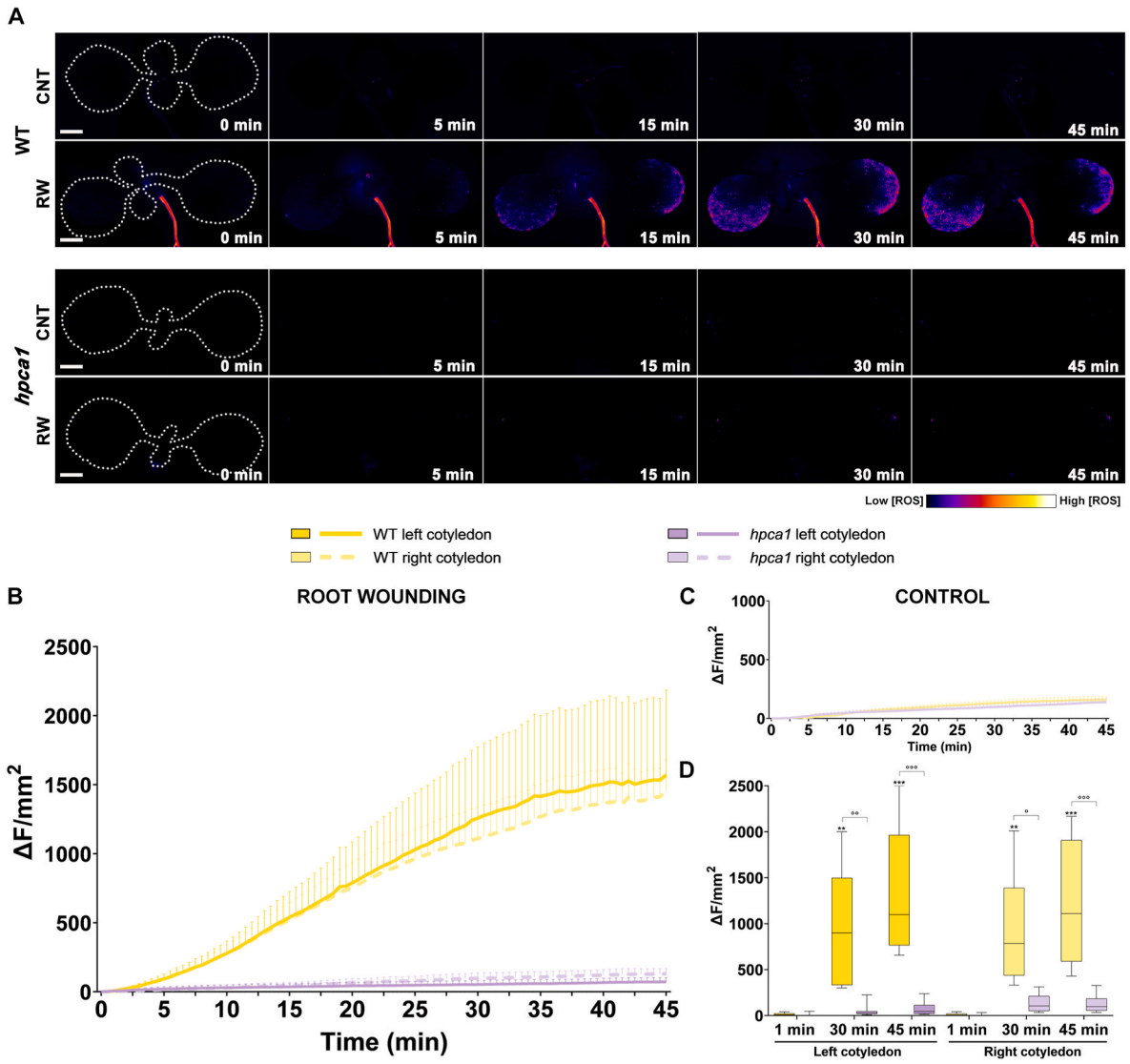

Fig. 2. Systemic ROS accumulation in response to root wounding (RW) in WT and *hpca1* Arabidopsis seedlings. (A) Seedlings were subjected to root wounding and ROS levels were imaged *in vivo* using CM-H_2DCFDA probe and wide-field fluorescence stereomicroscopy. Representative false-color images of control and wounded conditions are shown, at 0, 5, 15, 30 and 45 min after injury. Time-lapse acquisition was performed every 30 s for a total duration of 45 min. Scale bar = 1 mm. (B, C) Quantification of fluorescence levels, expressed as $\Delta F/mm^2$, over time in left and right cotyledons of wounded seedlings (B) and in control conditions (C). (D) Statistical analysis of ROS accumulation in left and right cotyledons at 1, 30 and 45 min post-injury. Median values are reported in the boxplot, as well as minimum and maximum values ($n = 12$). Comparisons within each genotype versus 1 min baseline were performed by one-way ANOVA followed by Dunnett's test (indicated by *), while between-genotype comparisons at the same time point and cotyledon were performed using unpaired *t*-test (indicated by °). Significant levels are reported: *, $° p \leq 0.05$; **, $° p \leq 0.01$; ***, $° p \leq 0.001$. Non-significant differences are not shown. (For interpretation of the references to color in this figure legend, the reader is referred to the Web version of this article.)

3.2. hpca1 mutant seedlings exhibit impaired wounding- and H_2O_2-triggered stomatal closure

Mechanical wounding is known to induce rapid local and systemic stomatal closure in Arabidopsis seedlings, contributing to whole-plant acclimation to stress (Devireddy et al., 2020; Fichman and Mittler, 2021; Fraudentali et al., 2023). Given the established role of HPCA1 as an extracellular H_2O_2 sensor and its constitutive expression in guard cells, we investigated whether HPCA1 participates in the systemic stomatal response to wounding. Accordingly, 7-day-old WT and *hpca1* seedlings were subjected to cotyledonary-leaf or root wounding, or treated with 100 μM H_2O_2, and stomatal aperture was quantified at 5, 15, 30 min and 1 h (Fig. 3). Additional 3 and 24 h time points for cotyledonary-leaf and root wounding are provided in supplementary data (Fig. S1).

Consistent with previous reports (Fraudentali et al., 2021, 2023), WT seedlings exhibited time-dependent stomatal closure in response to both cotyledonary-leaf and root wounding (Fig. 3A and B). Following leaf injury, stomata in the wounded cotyledon (local response) started to close within 5 min and reached approximately 70% closure by 1 h (Fig. 3A). In the unwounded cotyledon (distal response), stomatal closure was initiated 30 min after injury, peaking at approximately 65% by 1 h (Fig. 3A). Following root wounding, WT stomata started to close after 5 min and reached approximately 64% by 1 h (Fig. 3B). Similar to wounding, H_2O_2 treatment triggered time-dependent stomatal closure in WT seedlings, starting at 5 min and peaking at approximately 40% by 1 h (Fig. 3C), confirming the ability of guard cells to respond directly to extracellular ROS signals. In contrast, *hpca1* seedlings failed to close their stomata in response to either wounding or H_2O_2 treatment, with stomatal aperture values remaining comparable to those measured under control conditions throughout the time-course (Fig. 3). Together, these findings identify HPCA1 as a key component of the molecular

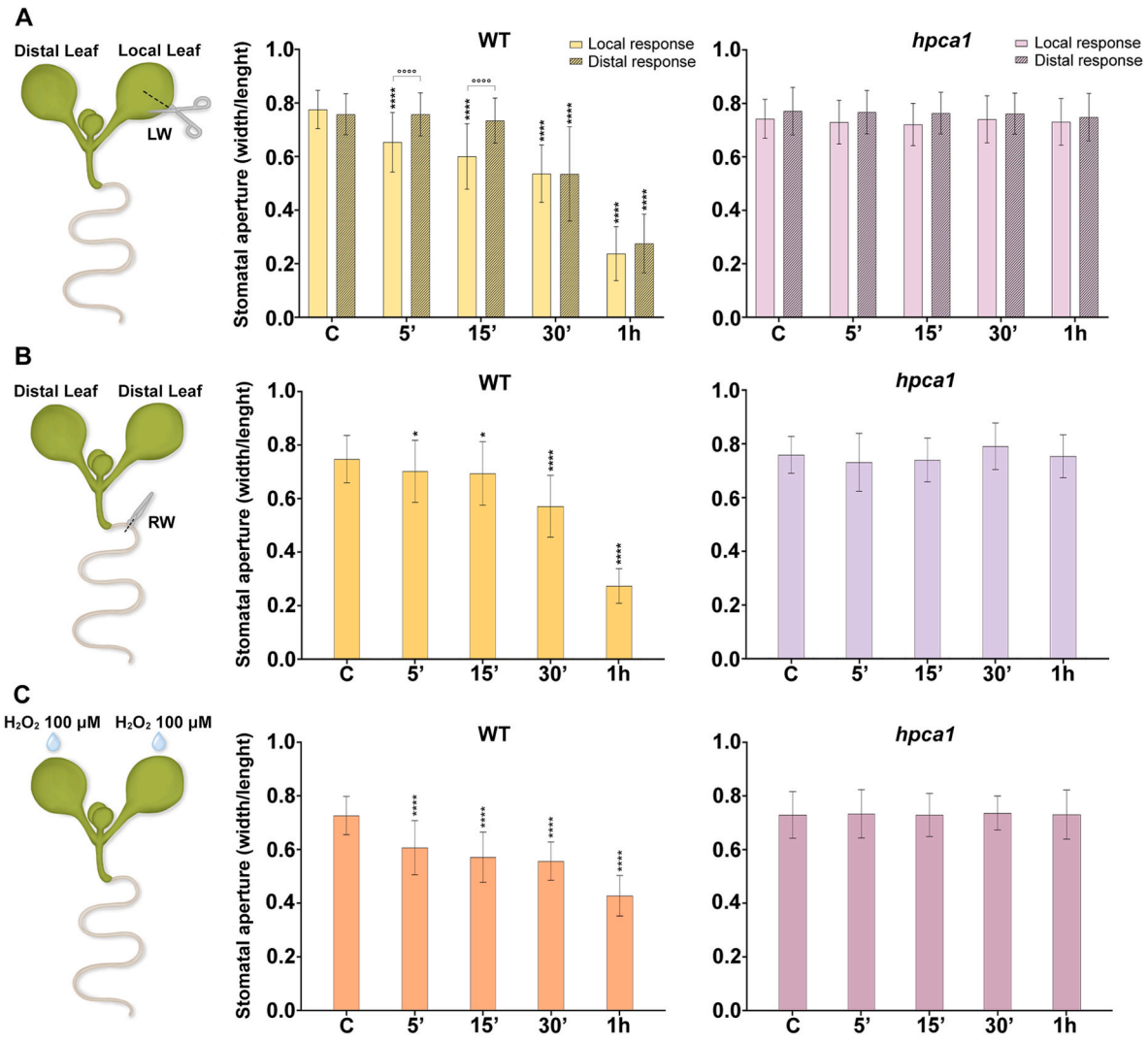

Fig. 3. Stomatal response of 7-day-old WT and *hpca1* seedlings to cotyledonary-leaf wounding (LW) or root wounding (RW) and H_2O_2 treatments. Stomatal aperture was assessed at 5, 15, 30 min and 1 h after wounding or treatment. (A) Following cotyledonary-leaf wounding, stomatal aperture was measured separately in wounded cotyledons (local response) and unwounded cotyledons (distal response). (B) Following root wounding, and (C) 100 µM H_2O_2 treatment, stomatal aperture was quantified using stomata randomly chosen from both cotyledons of each seedling. Graphs show mean ± SD ($n = 15$). Statistical significance was determined by one-way ANOVA followed by Dunnett's test (indicated by *), comparing control -C- and wounded or treated samples within each genotype. For leaf wounding (local and distal tissues), comparisons between cotyledons at the same time point were performed using unpaired Student's *t*-test (indicated by °). Significance levels: *, $p \leq 0.05$; ****, °$p \leq 0.0001$. Non-significant differences are not indicated.

pathway linking wound-induced and ROS-dependent signals to stomatal closure. Moreover, analysis of stomatal size revealed no significant differences between WT and *hpca1* seedlings (Fig. S2B), confirming that the observed differences in stomatal closure are due to functional effects of HPCA1 rather than inherent differences in stomatal characteristics between the genotypes. To further exclude a size-dependent bias, we additionally analyzed the 1 h H_2O_2 dataset by grouping stomata according to guard cell pair length (>11.5 µm and <11.5 µm; Fig. S2C). Both size groups of each genotype responded similarly to H_2O_2, indicating that the observed response to H_2O_2 is independent of guard cell pair length within the mature stomatal population.

3.3. Absence of HPCA1 impairs ROS accumulation in guard cells in response to wounding and H_2O_2

Once it was established that *hpca1* seedlings do not show a WT-like systemic ROS burst in response to cotyledonary-leaf or root wounding, and we observed that *hpca1* seedlings exhibited altered stomatal responses following both cotyledonary-leaf and root wounding, we next examined whether HPCA1 contributes to ROS dynamics at the level of guard cells. To this end, ROS accumulation was observed *in vivo* in 7-day old WT and *hpca1* seedlings using LSCM and the fluorescent probe CM-H_2DCFDA, upon cotyledonary-leaf or root wounding, as well as after 100 µM H_2O_2. Quantification was performed at 5 min and 1 h (Fig. 4).

Consistent with previous reports (Fraudentali et al., 2023), in WT seedlings, cotyledonary-leaf wounding induced a significant increase in ROS-associated fluorescence in guard cells of the wounded cotyledon within 5 min after injury, while no increase was yet detectable in the distal cotyledon (Fig. 4A and B). At 1 h after wounding, ROS levels had risen in both the wounded and distal cotyledons, reaching comparable intensity (Fig. 4C and D). Following root wounding, ROS-associated fluorescence in WT cotyledon guard cells increased rapidly by 5 min, exceeding the early response observed after leaf wounding, and persisted at high levels after 1 h (Fig. 4). Similarly, treatment with 100 µM H_2O_2 triggered a time-dependent ROS accumulation in WT guard cells, with fluorescence levels peaking at 1 h after application (Fig. 4). Guard cells of *hpca1* seedlings displayed slightly higher basal ROS levels compared to WT and failed to exhibit a significant increase in

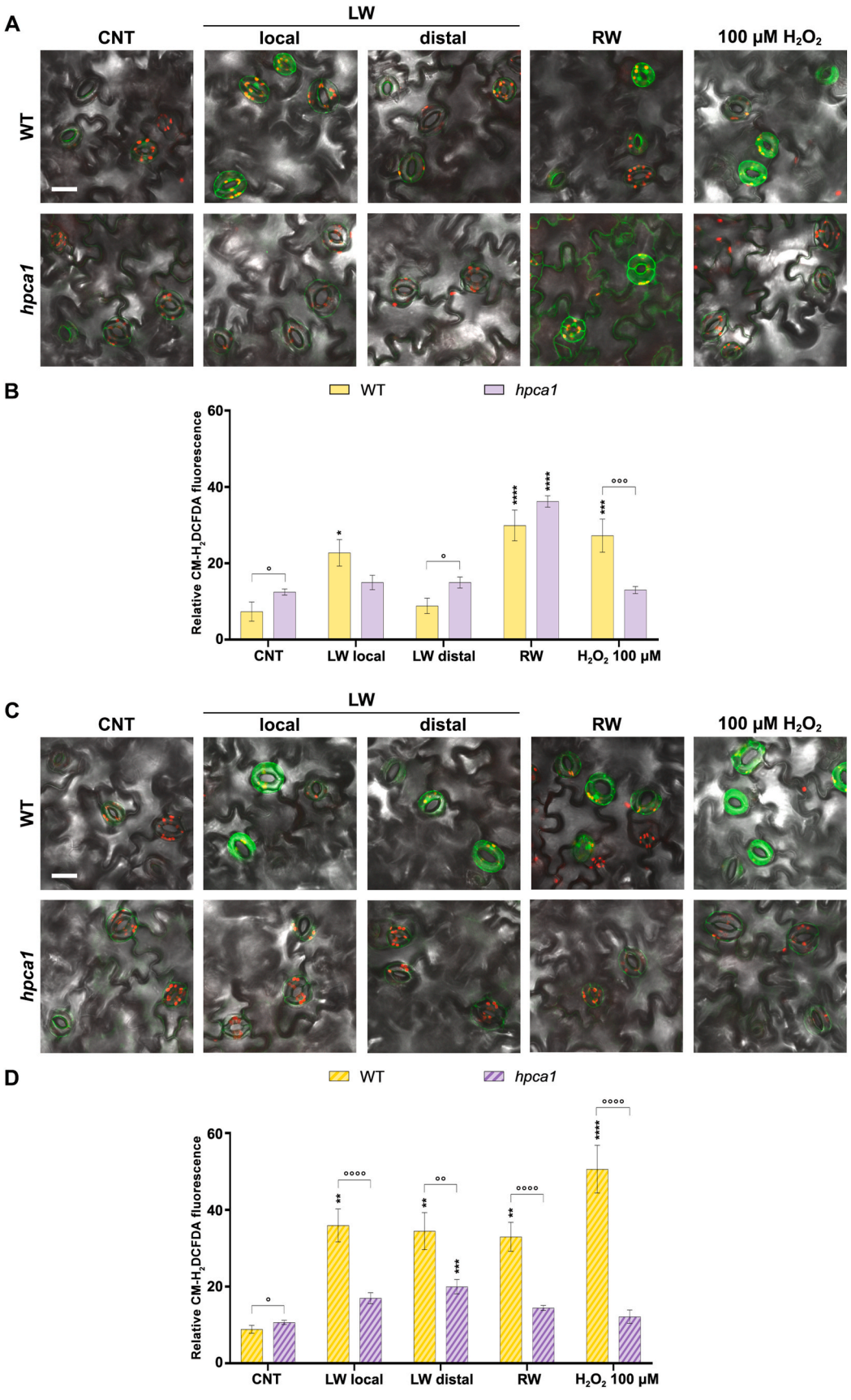

(caption on next page)

Fig. 4. ROS accumulation in stomata guard cells of 7-day-old WT and *hpca1* Arabidopsis seedlings, following cotyledonary-leaf or root wounding, and H_2O_2 treatment. (A, C) Images of stomata guard cells of both seedlings were acquired using LSCM and CM-H_2DCFDA staining 5 min (A) or 1 h (C) after wounding or treatment. Representative images of stomata of control conditions (CNT), wounded cotyledons (LW local), unwounded cotyledons (LW distal), root wounded seedlings (RW), and 100 μM H_2O_2-treated seedlings are reported. Scale bar = 10 μm. (B, D) Quantification of CM-H_2DCFDA relative fluorescence intensity in guard cells at 5 min (B) or 1 h (D) is shown in the graph, reporting means ± SEM (n = 15). Comparisons within each genotype versus CNT were performed by one-way ANOVA followed by Dunnett's test (indicated by *), while between-genotype comparisons were performed using unpaired *t*-test (indicated by °). Significant levels are reported: *, ° $p \leq 0.05$; **, ° $p \leq 0.01$; ***, ° $p \leq 0.001$; ****, °$p \leq 0.0001$. Non-significant differences are not shown.

ROS-associated fluorescence in response to either wounding or H_2O_2 treatment, with ROS levels remaining comparable to control conditions at most analyzed time points (Fig. 4). Exceptions included a transient increase 5 min after root wounding (Fig. 4A and B), which quickly returned to basal levels (Fig. 4C, D), and a low-level rise in fluorescence in the distal cotyledon 1 h after cotyledonary-leaf wounding (Fig. 4C and D), although levels remained substantially lower than those measured in WT seedlings under the same conditions. Taken together, these findings demonstrate that HPCA1 is fundamental for ROS accumulation in guard cells in response to wounding and exogenous H_2O_2.

4. Discussion

Rapid integration of locally perceived stimuli into systemic signaling responses is central to plant acclimation under adverse environmental conditions (Kollist et al., 2019; Myers et al., 2024). In this context, the identification of HPCA1 as a PM H_2O_2 receptor advanced our understanding of ROS-triggered Ca^{2+} signaling (Wu et al., 2020). In this study, we investigated the specific role of HPCA1 in stress perception, systemic ROS accumulation, and the regulation of systemic stomatal closure in response to wounding and exogenous H_2O_2 application, using Arabidopsis at the cotyledon stage. *In vivo* whole-seedling fluorescence analyses (Figs. 1 and 2) revealed that *hpca1* seedlings exhibited an altered ROS accumulation both locally and distally following wounding, with fluorescence levels strongly reduced compared with WT, indicating that HPCA1 plays a critical role for the establishment of wound-induced ROS signals at the systemic level. Interestingly, while a low but detectable ROS-associated fluorescence was still observed in *hpca1* seedlings following cotyledonary-leaf wounding, no fluorescence increase was detected after root wounding. A possible explanation for the different responses observed after cotyledonary-leaf and root wounding is that cotyledon excision generates a stronger local ROS burst that remains partially detectable even in the absence of HPCA1-dependent amplification, whereas root pinching likely produces a rapid but more transient signal that quickly reaches the shoot along the root–shoot axis and may therefore require HPCA1-mediated reinforcement to be sustained. This result suggests that, in seedlings, HPCA1 is not merely involved in downstream decoding of ROS signals, but is also required for sustaining or amplifying ROS accumulation itself. Given the previously described positive feedback loop between apoplastic ROS production and Ca^{2+} influx (Miller et al., 2009), the absence of HPCA1 may disrupt this auto-propagating mechanism, preventing the reinforcement of RBOH activity and thereby impairing the systemic ROS burst. In this scenario, extracellular ROS perception by HPCA1 would be necessary to maintain Ca^{2+} influx, which in turn sustains NADPH oxidase-dependent ROS production, enabling long-distance signal propagation. Our findings are consistent with previous work which reported that HPCA1 is required for systemic ROS and Ca^{2+} signaling in adult plants exposed to several abiotic and biotic stresses, including HL, and pathogen attack (Fichman et al., 2022). Notably, however, wound-induced systemic ROS signal propagation in adult plants was shown to occur largely independently of HPCA1 (Fichman et al., 2022). This apparent contrast, in light of our findings in seedlings, may derive from differences in the architecture of systemic signaling networks across developmental stages. Indeed, the differential contribution of HPCA1-dependent ROS signaling at the cotyledon stage likely reflects distinct developmental contexts along the seedling axis. Stress signaling pathways undergo substantial remodeling during plant development, with younger tissues often displaying reduced redundancy and a greater reliance on individual signaling components (Rankenberg et al., 2021). Cotyledons, hypocotyl, and roots originate from embryonic structures and retain specific anatomical, physiological, and hormonal characteristics, whereas the shoot apex undergoes post-embryonic organogenesis with dynamic meristematic activity. These developmental differences likely influence both ROS production and perception, explaining why HPCA1 plays a more central role in the ROS–Ca^{2+} signaling network of cotyledons, acting as a critical hub for ROS burst amplification. As development progresses, it is possible that additional signaling components and pathways in adult leaves provide stress-specific and partially redundant mechanisms that sustain ROS accumulation even in the absence of HPCA1.

The altered wound-induced systemic ROS accumulation observed in *hpca1* seedlings raises the question of whether impaired ROS signaling compromises downstream defense responses. Stomatal regulation is among the most extensively studied systemic responses and provides a rapid, quantifiable physiological output that integrates upstream ROS and Ca^{2+} signaling pathways and is established within minutes of stress perception (Suzuki and Mittler, 2012; Vega-Muñoz et al., 2020). Stomatal modulation analyses in *hpca1* seedlings revealed that they failed to respond to both wounding and H_2O_2 treatment (Fig. 3). These results indicate that HPCA1 represents a key component of the molecular pathway leading to stomatal closure triggered by mechanical injury and extracellular ROS accumulation, and are consistent with those reported by Wu and colleagues (2020) in response to exogenous H_2O_2.

In interpreting these results, it is important to consider the developmental context of the experimental system. Cotyledons provide a relatively homogeneous and developmentally informative tissue for stomatal analyses, as stomatal progression in this tissue is rapid and more coordinated than in expanding true leaves (Geisler and Sack, 2002), where multiple developmental stages continuously coexist. At 7 days after germination, the cotyledon epidermis contains both developing and fully differentiated stomata; however, our analysis was restricted to stomata with a clearly visible pore, thereby ensuring that only mature, physiologically active stomata were quantified. Variability in stomatal size within cotyledons at this stage likely reflects asynchronous developmental timing rather than incomplete differentiation. Combined with the lack of significant differences in stomatal size between WT and *hpca1* (Fig. S2B), this supports the conclusion that the impaired stomatal closure observed in *hpca1* seedlings is due to the functional absence of HPCA1 rather than differences in stomatal development within or between genotypes. Importantly, the supplementary analysis based on guard cell pair length in the 1 h H_2O_2 dataset (Fig. S2C) indicated that stomata from both size groups respond similarly, supporting the conclusion that the phenotype is unlikely to be explained by size-related heterogeneity within the mature stomatal population.

The involvement of HPCA1 in stomatal regulation is further supported by our analysis of ROS accumulation at the guard cells level (Fig. 4). Using CM-H_2DCFDA, we observed that wounding induces a rapid and transient increase in ROS levels in guard cells of WT seedlings, in line with the propagation of a systemic ROS burst (consistent with previous findings, Fraudentali et al., 2023). Similarly, exogenous H_2O_2 application triggered a strong ROS accumulation in guard cells, supporting the notion that extracellular ROS act as upstream signals for stomatal responses in seedlings. To ensure comparable guard cell opening before CM-H_2DCFDA loading, stomata were pre-opened using a standard opening solution applied uniformly across all samples, thereby

minimizing any potential differential effects of the opening solution among genotypes prior to treatment. In *hpca1* seedlings, ROS accumulation in guard cells was strongly compromised at both early and late time points following leaf wounding or H_2O_2 treatment, and at late time points after root wounding, indicating that HPCA1 is a key mediator of extracellular ROS perception and/or transduction in guard cells. Nonetheless, after root wounding, a transient increase in guard-cell ROS was detected in *hpca1* seedlings at early time points, but this signal was not sustained and was not accompanied by stomatal closure. By contrast, following cotyledonary-leaf wounding a low-level but significant rise in distal-cotyledon guard-cell fluorescence was observed in *hpca1* only at the 1 h time point. These observations are concordant with a model in which root-derived systemic signaling reaches distal guard cells more rapidly than cotyledon-derived signaling (see also the dynamics of stomatal responses, which show an earlier response after root wounding and a slower distal response after cotyledon wounding in WT seedlings, Fig. 3). This suggests that an initial systemic ROS signal can reach distal guard cells independently of HPCA1, whereas signal maintenance and functional decoding require HPCA1-dependent mechanisms. Furthermore, the transient but consistent ROS accumulation after root wounding may also reflect the distinct nature of the stress applied: in seedlings, roots must be pinched rather than cut, while cotyledons can be partially excised to create a wound. Our results are consistent with Fichman et al. (2022), who showed that mechanical pinching of adult leaves triggers ROS accumulation even in *hpca1* mutants. In line with this, we observed that pinching roots induces a transient ROS accumulation in *hpca1*, while cutting cotyledons generates a stronger ROS burst that can be sustained in WT seedlings through HPCA1-dependent amplification but rapidly decays in the absence of HPCA1.

A possible interpretation for our results is that HPCA1 is dispensable for the onset of the systemic ROS burst but is essential for local signal reinforcement. Previous studies have shown that HPCA1 mediates Ca^{2+} influx in response to extracellular H_2O_2 (Wu et al., 2020), a critical process for sustaining the positive interaction between Ca^{2+} signaling and ROS production. In the absence of HPCA1, the transient ROS accumulation observed shortly after root wounding may represent a passive or diffusion-driven signal that fails to trigger sufficient Ca^{2+} influx, preventing activation of downstream components required for sustained ROS production and stomatal closure. As a result, guard cells in *hpca1* seedlings appear unable to translate transient extracellular ROS cues into stable intracellular transduction pathways and physiological output. The failure of *hpca1* seedlings to close stomata despite transient ROS presence further indicates that ROS accumulation alone is insufficient to induce stomata responses without proper signal amplification and decoding. Notably, the slightly higher basal ROS levels observed in *hpca1* guard cells indicate an altered redox homeostasis, which may compromise the effective amplification and propagation of wound-induced ROS signals. Together, these findings support a model in which HPCA1 acts as a critical hub linking extracellular ROS perception to Ca^{2+}-dependent signal reinforcement, enabling maintenance of guard-cell ROS dynamics and the execution of systemic stomatal acclimation following stress perception.

Altogether, our results indicate that HPCA1 is essential for sustaining ROS-dependent systemic signaling in Arabidopsis at the cotyledon stage. Loss of HPCA1 disrupts this cascade, impairing the persistence of systemic ROS signals, guard-cell signal amplification and wound-induced stomatal acclimation. In this framework, future work will be essential to determine how HPCA1-dependent signaling interfaces with parallel and partially redundant pathways and how these interactions evolve across developmental stages and stress contexts.

5. Conclusions

Our results show that HPCA1 is essential for wound-induced systemic ROS signaling in Arabidopsis seedlings. In *hpca1*, ROS accumulation is compromised both at the site of wounding and in distal tissues, including guard cells, preventing the implementation of local and systemic stomatal closure. These results indicate that extracellular ROS perception by HPCA1 is required to maintain and propagate systemic ROS signals. By enabling coordinated ROS dynamics across tissues, HPCA1 ensures rapid physiological acclimation to wounding. This study highlights HPCA1 as a key mediator linking extracellular ROS perception to whole-seedling stress responses, providing new insights into the mechanisms controlling systemic signaling and stomatal regulation in early plant development.

CRediT authorship contribution statement

I. Fraudentali: Writing – original draft, Investigation, Data curation, Conceptualization. **A. Furlani:** Writing – original draft, Investigation, Data curation. **M. Gagliano:** Writing – original draft, Investigation, Data curation. **A. Cona:** Writing – review & editing, Supervision, Funding acquisition, Conceptualization.

Funding sources

This work was supported by the Italian "Ministero dell'Università e della Ricerca-MUR" (PRIN, 2022 project contract no. 2022WLZ4HB), the Italian "Ministero dell'Università e della Ricerca-MUR" (Italy departments of excellence 2023-2027 to the dept. of Science, Univ. Roma Tre – ARTICOLO 1, COMMI 314–337 LEGGE 232/2016), and Università degli Studi "Roma Tre", Italy.

Declaration of competing interest

The authors declare that they have no known competing financial interests or personal relationships that could have appeared to influence the work reported in this paper.

Acknowledgements

We thank Prof. Zhen-Ming Pei (Department of Biology, Duke University, Durham, NC, USA) for generating the *hpca1* mutant line used in this study, and Prof. Alex Costa (Department of Biosciences, University of Milan, Milan, Italy) for kindly providing these seeds to us. The authors acknowledge the support of NBFC to the University of Roma Tre, funded by the Italian Ministry of University and Research, PNRR, Missione 4 Componente 2, "Dalla ricerca all'impresa", Investimento 1.4, Project CN00000033. The authors thank the funding sources cited above for the support of the work presented in this manuscript.

Appendix A. Supplementary data

Supplementary data to this article can be found online at https://doi.org/10.1016/j.jplph.2026.154773.

Data availability

Data will be made available on request.

References

Devireddy, A.R., Arbogast, J., Mittler, R., 2020. Coordinated and rapid whole-plant systemic stomatal responses. New Phytol. 225 (1), 21–25. https://doi.org/10.1111/nph.16143.

Fichman, Y., Mittler, R., 2020. Rapid systemic signaling during abiotic and biotic stresses: is the ROS wave master of all trades? Plant J.: Cell. Mol. Biol. (Sarreguemines, Fr., Online) 102 (5), 887–896. https://doi.org/10.1111/tpj.14685.

Fichman, Y., Mittler, R., 2021. A systemic whole-plant change in redox levels accompanies the rapid systemic response to wounding. Plant Physiol. 186 (1), 4–8. https://doi.org/10.1093/plphys/kiab022.

Fichman, Y., Zandalinas, S.I., Peck, S., Luan, S., Mittler, R., 2022. HPCA1 is required for systemic reactive oxygen species and calcium cell-to-cell signaling and plant acclimation to stress. Plant Cell 34 (11), 4453–4471. https://doi.org/10.1093/plcell/koac241.

Fraudentali, I., Ghuge, S.A., Carucci, A., Tavladoraki, P., Angelini, R., Rodrigues-Pousada, R.A., Cona, A., 2020. Developmental, hormone- and stress-modulated expression profiles of four members of the Arabidopsis copper-amine oxidase gene family. Plant Physiol. Biochem. 147, 141–160. https://doi.org/10.1016/j.plaphy.2019.11.037. Epub 2019 Nov 25. PMID: 31862580.

Fraudentali, I., Pedalino, C., D'Incà, R., Tavladoraki, P., Angelini, R., Cona, A., 2023. Distinct role of AtCuAOβ- and RBOHD-driven H_2O_2 production in wound-induced local and systemic leaf-to-leaf and root-to-leaf stomatal closure. Front. Plant Sci. 14, 1154431. https://doi.org/10.3389/fpls.2023.1154431.

Fraudentali, I., Pedalino, C., Tavladoraki, P., Angelini, R., Cona, A., 2021. A new player in jasmonate-mediated stomatal closure: the *Arabidopsis thaliana* copper amine oxidase β. Cells 10 (12), 3399. https://doi.org/10.3390/cells10123399.

Geisler, M.J., Sack, F.D., 2002. Variable timing of developmental progression in the stomatal pathway in Arabidopsis cotyledons. New Phytol. 153, 469–476. https://doi.org/10.1046/j.0028-646X.2001.00332.x.

Guo, S., Hu, X., Yu, F., Mu, L., 2024. Heat waves coupled with nanoparticles induce yield and nutritional losses in rice by regulating stomatal closure. ACS Nano 18 (22), 14276–14289. https://doi.org/10.1021/acsnano.3c13165.

Johns, S., Hagihara, T., Toyota, M., Gilroy, S., 2021. The fast and the furious: rapid long-range signaling in plants. Plant Physiol. 185 (3), 694–706. https://doi.org/10.1093/plphys/kiaa098.

Kollist, H., Zandalinas, S.I., Sengupta, S., Nuhkat, M., Kangasjärvi, J., Mittler, R., 2019. Rapid responses to abiotic stress: priming the landscape for the signal transduction network. Trends Plant Sci. 24 (1), 25–37. https://doi.org/10.1016/j.tplants.2018.10.003.

Kouhen, M., Dimitrova, A., Scippa, G.S., Trupiano, D., 2023. The course of mechanical stress: types, perception, and plant response. Biology 12 (2), 217. https://doi.org/10.3390/biology12020217.

Ladeynova, M., Kuznetsova, D., Mudrilov, M., Vodeneev, V., 2023. Integration of electrical signals and phytohormones in the control of systemic response. Int. J. Mol. Sci. 24 (1). https://doi.org/10.3390/ijms24010847.

Lawson, T., Matthews, J., 2020. Guard cell metabolism and stomatal function. Annu. Rev. Plant Biol. 71, 273–302. https://doi.org/10.1146/annurev-arplant-050718-100251.

Lew, T.T.S., Koman, V.B., Silmore, K.S., Seo, J.S., Gordiichuk, P., Kwak, S.-Y., Park, M., Ang, M.C.-Y., Khong, D.T., Lee, M.A., Chan-Park, M.B., Chua, N.-H., Strano, M.S., 2020. Real-time detection of wound-induced H_2O_2 signalling waves in plants with optical nanosensors. Nat. Plants 6 (4), 404–415. https://doi.org/10.1038/s41477-020-0632-4.

Liu, H., Song, S., Zhang, H., Li, Y., Niu, L., Zhang, J., Wang, W., 2022. Signaling transduction of ABA, ROS, and Ca^{2+} in plant stomatal closure in response to drought. Int. J. Mol. Sci. 23 (23). https://doi.org/10.3390/ijms232314824.

Mansoor, S., Ali Wani, O., Lone, J.K., Manhas, S., Kour, N., Alam, P., Ahmad, A., Ahmad, P., 2022. Reactive oxygen species in plants: from source to sink. Antioxidants 11 (2), 225. https://doi.org/10.3390/antiox11020225.

Miller, G., Schlauch, K., Tam, R., Cortes, D., Torres, M.A., Shulaev, V., Dangl, J.L., Mittler, R., 2009. The plant NADPH oxidase RBOHD mediates rapid systemic signaling in response to diverse stimuli. Sci. Signal. 2 (84). https://doi.org/10.1126/scisignal.2000448 ra45.

Mittler, R., Jones, D.P., 2024. The redox code of plants. Plant Cell Environ. 47 (8), 2821–2829. https://doi.org/10.1111/pce.14787.

Morales, J., Kadota, Y., Zipfel, C., Molina, A., Torres, M.-A., 2016. The Arabidopsis NADPH oxidases *RbohD* and *RbohF* display differential expression patterns and contributions during plant immunity. J. Exp. Bot. 67 (6), 1663–1676. https://doi.org/10.1093/jxb/erv558.

Murashige, T., Skoog, F., 1962. A revised medium for rapid growth and bio assays with tobacco tissue cultures. Physiol. Plantarum 15 (3), 473. https://doi.org/10.1111/j.1399-3054.1962.tb08052.x.

Myers, R.J., Peláez-Vico, M.Á., Fichman, Y., 2024. Functional analysis of reactive oxygen species-driven stress systemic signalling, interplay and acclimation. Plant Cell Environ. 47 (8), 2842–2851. https://doi.org/10.1111/pce.14894.

Paes de Melo, B., Carpinetti, P. de A., Fraga, O.T., Rodrigues-Silva, P.L., Fioresi, V.S., de Camargos, L.F., Ferreira, M.F. da S., 2022. Abiotic stresses in plants and their markers: a practice view of plant stress responses and programmed cell death mechanisms. Plants 11 (9), 1100. https://doi.org/10.3390/plants11091100.

Peláez-Vico, M.Á., Fichman, Y., Zandalinas, S.I., Foyer, C.H., Mittler, R., 2024. ROS are universal cell-to-cell stress signals. Curr. Opin. Plant Biol. 79, 102540. https://doi.org/10.1016/j.pbi.2024.102540.

Peláez-Vico, M.Á., Fichman, Y., Zandalinas, S.I., Van Breusegem, F., Karpiński, S.M., Mittler, R., 2022. ROS and redox regulation of cell-to-cell and systemic signaling in plants during stress. Free Radical Biol. Med. 193 (Pt 1), 354–362. https://doi.org/10.1016/j.freeradbiomed.2022.10.305.

Planas-Riverola, A., Markaide, E., Caño-Delgado, A.I., 2021. New role for LRR-receptor kinase in sensing of reactive oxygen species. Trends Plant Sci. 26 (2), 102–104. https://doi.org/10.1016/j.tplants.2020.11.011.

Rankenberg, T., Geldhof, B., van Veen, H., Holsteens, K., Van de Poel, B., Sasidharan, R., 2021. Age-dependent abiotic stress resilience in plants. Trends Plant Sci. 26 (7), 692–705. https://doi.org/10.1016/j.tplants.2020.12.016.

Rodrigues, O., Shan, L., 2022. Stomata in a state of emergency: H_2O_2 is the target locked. Trends Plant Sci. 27 (3), 274–286. https://doi.org/10.1016/j.tplants.2021.10.002.

Shang, Y., Dai, C., Lee, M.M., Kwak, J.M., Nam, K.H., 2016. BRI1-Associated receptor kinase 1 regulates guard cell ABA signaling mediated by open stomata 1 in *Arabidopsis*. Mol. Plant 9 (3), 447–460. https://doi.org/10.1016/j.molp.2015.12.014.

Suzuki, N., Mittler, R., 2012. Reactive oxygen species-dependent wound responses in animals and plants. Free Radical Biol. Med. 53 (12), 2269–2276. https://doi.org/10.1016/j.freeradbiomed.2012.10.538.

Terrón-Camero, L.C., Peláez-Vico, M.Á., Rodríguez-González, A., Del Val, C., Sandalio, L. M., Romero-Puertas, M.C., 2022. Gene network downstream plant stress response modulated by peroxisomal H_2O_2. Front. Plant Sci. 13, 930721. https://doi.org/10.3389/fpls.2022.930721.

Vega-Muñoz, I., Duran-Flores, D., Fernández-Fernández, Á.D., Heyman, J., Ritter, A., Stael, S., 2020. Breaking bad news: dynamic molecular mechanisms of wound response in plants. Front. Plant Sci. 11, 610445. https://doi.org/10.3389/fpls.2020.610445.

Wang, P., Liu, W.-C., Han, C., Wang, S., Bai, M.-Y., Song, C.-P., 2024. Reactive oxygen species: multidimensional regulators of plant adaptation to abiotic stress and development. J. Integr. Plant Biol. 66 (3), 330–367. https://doi.org/10.1111/jipb.13601.

Wang, P., Song, C.-P., 2008. Guard-cell signalling for hydrogen peroxide and abscisic acid. New Phytol. 178 (4), 703–718. https://doi.org/10.1111/j.1469-8137.2008.02431.x.

Wu, F., Chi, Y., Jiang, Z., Xu, Y., Xie, L., Huang, F., Wan, D., Ni, J., Yuan, F., Wu, X., Zhang, Y., Wang, L., Ye, R., Byeon, B., Wang, W., Zhang, S., Sima, M., Chen, S., Zhu, M., et al., 2020. Hydrogen peroxide sensor HPCA1 is an LRR receptor kinase in *Arabidopsis*. Nature 578 (7796), 577–581. https://doi.org/10.1038/s41586-020-2032-3.

Zandalinas, S.I., Fichman, Y., Mittler, R., 2020. Vascular bundles mediate systemic reactive oxygen signaling during light stress. Plant Cell 32 (11), 3425–3435. https://doi.org/10.1105/tpc.20.00453.